Journal of Membrane Science, 73 (1992) 73-85
Elsevier Science Publishers B.V., Amsterdam

Gas separation processes in membrane absorber

A.B. Shelekhin[a] and **I.N. Beckman**[b]

[a] C*enter for Inorganic Membrane Studies, Chemical Engineering Department, Worcester Polytechnic Institute, Worcester, MA 01609 (USA)*
[c] C*hemical Engineering Department, Moscow State University, Moscow (Russia)*

The possibility of combining absorption and membrane gas separation processes in one integrated system is considered. Theoretical models for gas transport phenomena in membrane absorbers of different configurations are presented. A selectivity factor higher than 3000 was observed in experiments on a CO_2/CH_4 gas mixture separation, using a laboratory membrane absorber with polvinyltrimethylsilane asymmetric membranes and a solution of monoethanolamine in water as an absorbent.

Keywords: diffusion; facilitated transport; gas separations; liquid membranes; modules

Introduction

For several years numerous attempts have been made to bring the concept of the so called liquid membranes to commercialization. In spite of all the advantages exhibited by liquid membranes over polymeric ones, such as high permeability and selectivity [1-3], they have not been put into practice due to their poor mechanical stability. To overcome this drawback Sirkar et al. have developed the idea of preparing a membrane by placing liquid between two polymeric membranes [4, 5]. Even though the mechanical stability of such a system is good, the overall diffusion thickness (100-200/un) is too large to provide sufficient transmembrane fluxes. This idea was also developed in the work of Teramoto et al. [6]. They proposed to pump the liquid between polymeric membranes in a circulatory mode. The diffusional resistance in such a system decreased compared to a conventional liquid membrane design. That resulted in an increase of transmembrane flux, although at the price of process selectivity. The authors referred to such a system as a "moving liquid membrane". At the same time it was proposed by the present authors [7-9] to separate spatially the inlet and the outlet surfaces of the liquid membrane into different modules and to perform gas transport between them by the use of an absorption liquid. This approach led to the creation of the so-called "membrane absorber".

Recent developments in membrane module design have made it possible to create devices with an extremely high ratio of membrane area to module volume. At the same time asymmetric hollow fiber polymeric membranes with a very thin dense polymer layer have become commercially available. All these achievements have made it possible to create an artificial lung and gills based on hollow fiber membrane modules [10, 11]. Further development of the artificial lung concept necessarily leads to creation of an artificial "blood system" with absorption and desorption modules where an absorption liquid is separated from the gas phase by polymeric membranes. Such an artificial "blood system" demonstrates the flexibility common to natural blood systems, such as the ability to regulate the transport properties by controlling the blood flow rate.

The main objective of this paper is to provide experimental data and simulation results for a membrane absorber and its gas separation properties.

Theory

(1) Structural types of membrane absorbers

There are two main structural units in membrane absorber design:
- absorber module (Fig. la);
- desorber module (Fig. lb).

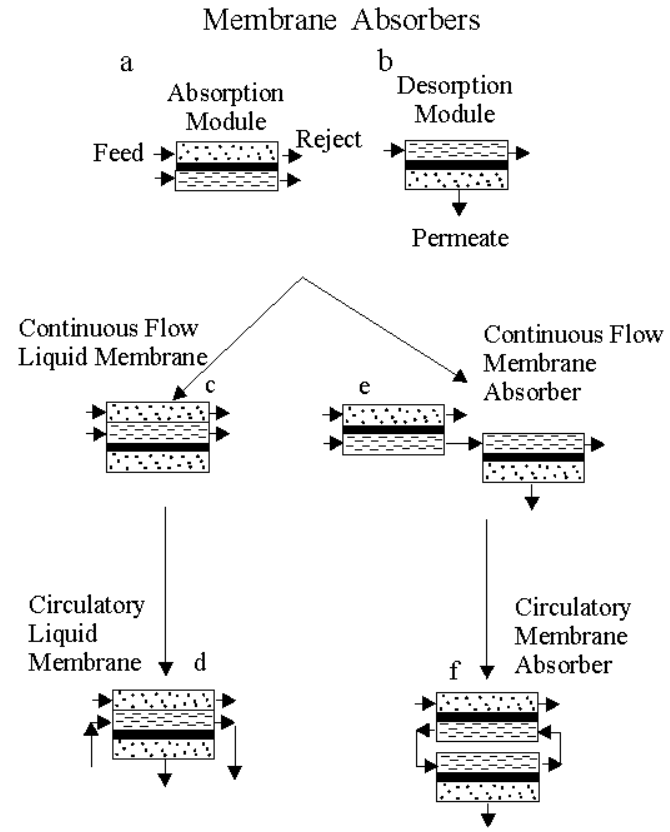

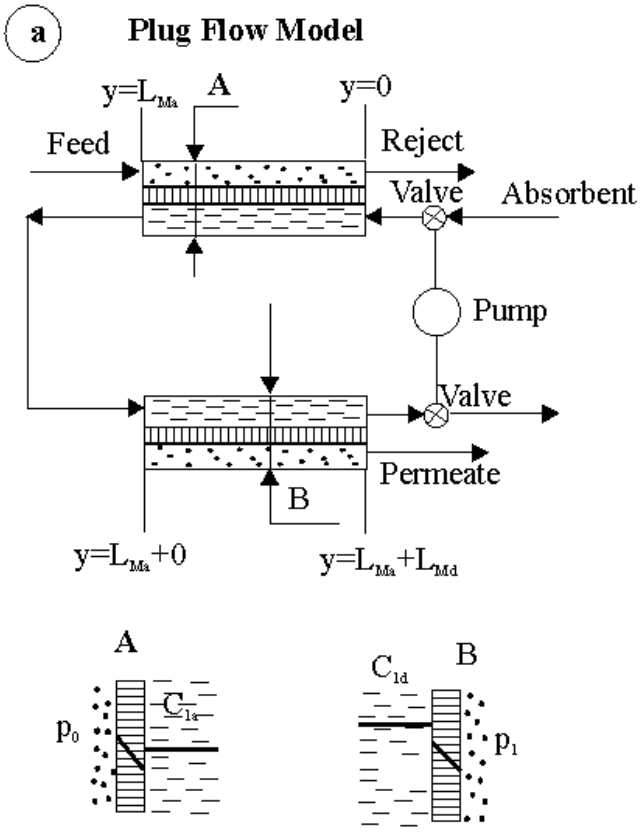

In an absorption module (Fig. la) a mixture of gases diffuses through a polymeric membrane and dissolves in the absorption liquid. By continuous pumping of fresh liquid into the module, the absorbent with the dissolved gas is continuously replaced by fresh degassed liquid. In the desorption module (Fig. lb) the absorbent saturated with gas is discharged through a polymeric membrane due to the concentration gradient across the membrane.

One can imagine at least four different ways of combining absorption and desorption modules into a single gas separation device. One of the possible structural types of membrane absorbers will lead to the so called "flowing liquid membranes" [6] (Fig. lc, d), while another one will lead to "membrane absorbers" (Fig. le, f).

Fig. 1. Structural types of membrane absorbers.

There are two principal types of membranes absorbers:

- the continuous flow membrane absorber (Fig.le);
- the circulatory membrane absorber (Fig. If).

In this study we will focus mainly on the characterization of membrane absorbers. More detailed information regarding the flowing liquid membranes may be found elsewhere [6].

(2) Plug-flow model

For better understanding of membrane absorber gas separation properties, we shall perform a simplified analysis of a membrane absorber operation under steady state conditions based on the following assumptions (Fig. 2a):

- distribution of the penetrant across the liquid is uniform;
- flow rate profile of the liquid is uniform;
- diffusion of the liquid component through the polymeric membrane does not affect the penetrant gas transfer rates in it;
- absorption of gas in the liquid follows Henry's law.

With the above assumptions the gas transport equations in the membrane absorber will be

$$\frac{dC_{1a}}{dy} = \frac{Q_{Ma}S_{Ma}}{\sigma_1 Q L_{Ma}}\left(p_0\sigma_1 - C_{1a}\right) \qquad 0 \le y \le L_{Ma}\,, \tag{1a}$$

Fig. 2. Schematics of membrane absorber for eqns. 1-21 (a) andforeqns. 22-36(b).

$$\frac{dC_{1d}}{dy} = \frac{Q_{Md}S_{Md}}{\sigma_1 Q L_{Md}} C_{1d} \qquad L_{Ma} \le y \le L_{Ma} + L_{Md}\,, \text{ (lb)}$$

Equations (la) and (lb) can be written in dimensionless form as

$$A_a \frac{d\Psi_{1a}}{d\xi} = 1 - \Psi_{1a}; \qquad 0 \le \xi \le 1 \qquad (2a)$$

$$A_d \frac{d\Psi_{1d}}{d\xi} = -\Psi_{1d}; \qquad 1 \le \xi \le \eta \qquad (2b)$$

where

$\psi_{1a} = C_{1a}/C_0$ $\psi_{1d} = C_{ld}/C_o$

$$A_a = \frac{\sigma_1 \Omega}{Q_{Ma} S_{Ma}}; \; A_d = \frac{\sigma_1 \Omega}{Q_{Md} S_{Md}}$$

$\eta=(L_{Ma}+L_{Md})/L_{Md}$; $\xi=y/L_{Ma}$; $C_0 = \sigma_1 p_0$

The solution of the ordinary differential eqns (2a) and (2b) has the following form

$$C_{1a} = C_0\left[1 - K_a \exp\left(-\frac{\xi}{A_a}\right)\right] \qquad (3a;$$

$$C_{1d} = C_0\left[1 - K_d \exp\left(-\frac{\xi}{A_d}\right)\right] \qquad (3b)$$

where K_a and K_d are the constants determined from the boundary conditions.

Continuous flow membrane absorber

In a continuous flow membrane absorber fresh liquid is being fed into the absorber module. It carries the penetrant, which has passed through the membrane, into the desorber module. The penetrant is then discharged out of the desorber module.

The boundary conditions in this case are

$$\xi=0,\ C_{la}=C_{la}(0) \qquad (4)$$

$$\xi=1,\ C_{la}=C_{ld}$$

where $C_{1a}(0)$ is the concentration of the penetrant at the membrane absorber inlet. Applying these conditions to eqns. (3) we get

$$K_a = \frac{C_0 - C_{1a}(0)}{C_0} \qquad (5a)$$

$$K_d = \frac{1 - \frac{C_0 - C_{1a}(0)}{C_0}\exp\left(-\frac{1}{A_a}\right)}{\exp\left(-\frac{1}{A_d}\right)} \qquad (5b)$$

The concentration profiles in the y-direction

$$C_{1a} = C_0\left[1 - \frac{C_0 - C_{1a}(0)}{C_0}\exp\left(-\frac{\xi}{A_a}\right)\right] \qquad 0<\xi<1 \qquad (6a)$$

$$C_{1d} = \frac{C_0\left[1 - \frac{C_0 - C_{1a}(0)}{C_0}\exp\left(-\frac{\xi}{A_a}\right)\right]}{\exp\left(-\frac{1}{A_d}\right)}\exp\left(-\frac{\xi}{A_d}\right) \qquad 1\le\xi\le\eta \qquad (6b)$$

The total transmembrane flow rate of the penetrant at the desorber outlet

$$J_d = \Omega[C_{ld}(\xi=l) - C_{ld}(\xi=\eta)] \quad (7)$$

If $A_\alpha = A_d = A$ then

$$J_d = \sigma_1 p_0 \Omega\left[1 - \frac{C_0 - C_{1a}(0)}{C_0}\exp\left(-\frac{1}{A}\right)\right]\left[1 - \exp\left(-\frac{1}{A}\right)\right] \quad (8)$$

If $C_{la}(0)=0$ then

$$J_d = \sigma_1 p_0 \Omega\left[1 - \exp\left(-\frac{1}{A}\right)\right]^2 \quad (9)$$

The limits for J_d are

$$\lim_{\Omega\to 0}(J_d) = 0 \quad \lim_{\Omega\to\infty}(J_d) = 0 \quad (10)$$

The selectivity factor is determined by the formula

$$\alpha(\Omega) = \frac{J_d^A / p_0^A}{J_d^B / p_0^B} = \frac{\alpha_1^A\left[1 - \exp\left(-\frac{1}{A^A}\right)\right]^2}{\alpha_1^B\left[1 - \exp\left(-\frac{1}{A^B}\right)\right]^2} \quad (11)$$

The limits for a are

$$\lim_{\Omega\to 0}(\alpha) = \frac{\sigma_1^A}{\sigma_1^B}; \quad \lim_{\Omega\to\infty}(\alpha) = \left(\frac{Q_M^A}{Q_M^B}\right)\frac{\sigma_1^A}{\sigma_1^B} \quad (12)$$

Circulatory membrane absorber

In a circulatory membrane absorber (Fig. If) the absorbent is circulating between the absorber and desorber modules. The main advantage of this modification is that the absorbent is not consumed in this operation regime.

The boundary conditions in this case are

$$\xi=0, \quad C_{1d}=C_{1a}; \qquad \xi=1, \quad C_{1a}=C_{1d} \quad (13)$$

Then

$$K_a = \frac{1 - \exp\left(\frac{\eta-1}{A_d}\right)}{\exp\left(-\frac{1}{A_a}\right) - \exp\left(\frac{\eta-1}{A_d}\right)} \quad (14)$$

$$K_d = \frac{\left[\exp\left(-\frac{1}{A_a}\right) - 1\right]\exp\left(\frac{\eta}{A_d}\right)}{\exp\left(-\frac{1}{A_a}\right) - \exp\left(\frac{\eta-1}{A_d}\right)}$$

The total flow rate of the penetrant from the desorber module is determined by

$$J_d = \sigma_1 p_0 \Omega K_d\left[\exp\left(-\frac{1}{A_d}\right) - \exp\left(-\frac{\eta}{A_d}\right)\right] \quad (15)$$

With $A_a = A_d = A$, the eqn. (15) may be rearranged

$$J_{\mathrm{d}} = \sigma_1 p_0 \Omega \frac{\left[1-\exp\left(-\frac{1}{A_{\mathrm{d}}}\right)\right]^2}{1-\exp\left(-\frac{2}{A}\right)} \tag{16}$$

The limits for J_d are

$$\lim_{\Omega\to 0}\left(J_{\mathrm{d}}\right)=0;\quad \lim_{\Omega\to\infty}\left(J_{\mathrm{d}}\right)=\frac{Q_{\mathrm{M}} p_0}{2} \tag{17}$$

One may see that the flow rate of permeate , the desorber module in a circulatory membrane absorber is 1/[1 - exp(-2/A)] times greaten than in a continuous flow membrane absorber. The selectivity factor in a circulatory membrane absorber is

$$\alpha(\Omega)=\frac{\sigma_1^{\mathrm{A}}\left[1-\exp\left(-\frac{1}{A^{\mathrm{A}}}\right)\right]^2\left[1-\exp\left(-\frac{2}{A^{\mathrm{B}}}\right)\right]}{\sigma_1^{\mathrm{B}}\left[1-\exp\left(-\frac{1}{A^{\mathrm{B}}}\right)\right]^2\left[1-\exp\left(-\frac{2}{A^{\mathrm{A}}}\right)\right]} \tag{18}$$

The limits for α are

$$\lim_{\Omega\to 0}(\alpha)=\frac{\sigma_1^{\mathrm{A}}}{\sigma_1^{\mathrm{B}}};\quad \lim_{\Omega\to\infty}(\alpha)=\frac{Q_{\mathrm{M}}^{\mathrm{A}}}{Q_{\mathrm{M}}^{\mathrm{B}}} \tag{19}$$

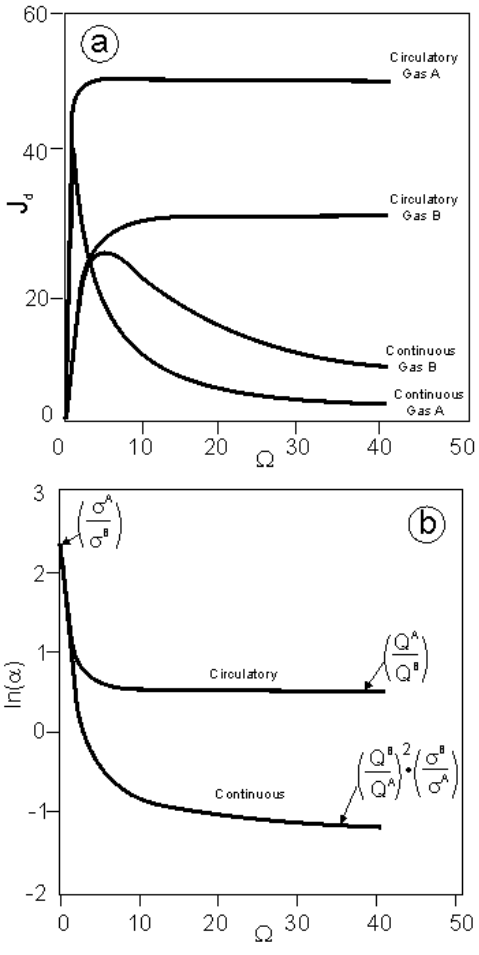

The effect of the liquid flow rate on the permeate flow rate and on the selectivity factor is represented in Figs. 3(a) and 3(b) for a model case. The results show, that an inversion of the selectivity factor may be observed with an increase of the absorbent flow rate if the following conditions are satisfied: Circulatory membrane absorber

$$\frac{\sigma_1^{\mathrm{A}}}{\sigma_1^{\mathrm{B}}}<1,\quad \frac{Q_{\mathrm{M}}^{\mathrm{A}}}{Q_{\mathrm{M}}^{\mathrm{B}}}>1 \tag{20}$$

or

$$\frac{\sigma_1^{\mathrm{A}}}{\sigma_1^{\mathrm{B}}}>1,\quad \frac{Q_{\mathrm{M}}^{\mathrm{A}}}{Q_{\mathrm{M}}^{\mathrm{B}}}<1$$

Continuous flow membrane absorber

$$\left(\frac{Q_{\mathrm{M}}^{\mathrm{A}}}{Q_{\mathrm{M}}^{\mathrm{B}}}\right)^2\frac{\sigma_1^{\mathrm{B}}}{\sigma_1^{\mathrm{A}}}>1,\quad \frac{\sigma_1^{\mathrm{A}}}{\sigma_1^{\mathrm{B}}}<1 \tag{21}$$

or

$$\left(\frac{Q_{\mathrm{M}}^{\mathrm{A}}}{Q_{\mathrm{M}}^{\mathrm{B}}}\right)^2\frac{\sigma_1^{\mathrm{B}}}{\sigma_1^{\mathrm{A}}}<1,\quad \frac{\sigma_1^{\mathrm{A}}}{\sigma_1^{\mathrm{B}}}>1$$

Fig. 3. Simulated permeate flow rate (a) and selectivity factors (b) in a membrane absorbers via absorbent flow rate: $Q_{\mathrm{M}}^{\mathrm{A}}$= 100, $Q_{\mathrm{M}}^{\mathrm{B}}$=30, σ_1^{A} = 100, σ_1^{B} = 10.

Even though the plug-flow model is a very effective approach for describing the gas separation properties of a membrane absorber, it

failed to predict quantitatively the experimental data on CO_2 permeation obtained in this work. Nevertheless, it gives us a better understanding of the limits imposed on the system under study. It follows from this analysis that at small absorbent flow rates, the selectivity of the process will be determined by the selectivity properties of the liquid, whereas at high absorbent flow rates the system will operate as a simple membrane module.

(3) Diffusion in lamellar media

The analysis of the gas separation properties of a membrane absorber by using the plug-flow model approximation is very fruitful (as it clearly shows the limits for selectivity and productivity in the device), but there are several restrictions on its applicability. First of all, the liquid flow profile is usually non-uniform. Second, the thickness of the membrane is considerably less than the thickness of the liquid layer. Consequently the concentration profile in the liquid will not be uniform. Thus, the plug-flow model is an idealized case when the rates of absorption/desorption processes are limited by the diffusion resistance of the polymeric membrane. An additional diffusion resistance of the absorption liquid will inevitably decrease the overall transmembrane flux. In order to develop a model which better describes the processes occurring in the real system, the following assumptions have been made:

- liquid flow rate profile is uniform;
- diffusion of the penetrant in the axial direction is negligible;
- diffusion of the liquid component through the polymeric membrane does not affect the penetrant gas transfer rates in it;
- absorption of gas in the liquid follows Henry's law.

Let us consider the case where the liquid is packed between two flat sheet membranes with flow in the y-direction. Depending on the penetrant concentration in the liquid and gas pressure outside the membranes, the module will act as an absorption or desorption module.

In general, absorption or desorption processes in such a system are to be considered as a two-dimensional problem. But with the first two assumptions made, it can be reduced to a problem of unsteady-state one-dimensional diffusion in a lamellar medium (Fig. 2b).

The system of differential equations for gas diffusion in three layered media is

$$\frac{\partial C_1}{\partial t} = D_{\mathrm{M}} \frac{\partial^2 C_1}{\partial x^2}, \quad 0 < x_1 < h_1 \tag{22a}$$

$$\frac{\partial C_2}{\partial t} = -\theta_{\mathrm{Y}} \frac{\partial C_2}{\partial y} + D_{\mathrm{l}} \frac{\partial^2 C_2}{\partial x_2^2}, \quad 0 < x_2 < h_2 \tag{22b}$$

$$\frac{\partial C_3}{\partial t} = D_{\mathrm{M}} \frac{\partial^2 C_3}{\partial x_3^2}, \quad 0 < x_3 < h_3 \tag{22c}$$

Assuming steady state, $h_1 = h3 = h_{\mathrm{M}}$, and $h_2 = h_1$, eqns. (22a) and (22c) can be rewritten as

$$0 = D_{\mathrm{M}} \frac{\partial^2 C_{\mathrm{M}}}{\partial x_{\mathrm{M}}^2}, \quad 0 < x_{\mathrm{M}} < h_{\mathrm{M}} \tag{23a}$$

and eqn. (22b) is written as

$$0 = \theta_{\mathrm{Y}} \frac{\partial C_1}{\partial y} + D_{\mathrm{l}} \frac{\partial^2 C_1}{\partial x_1^2}, \quad 0 < x_1 < h_1 \tag{23b}$$

To rearrange eqn. (22b) we have to take into consideration that if the liquid flow profile is uniform, as assumed, then the following equation is true

$$\frac{\mathrm{d}\, y}{\mathrm{d}\, \tau} = \theta_{\mathrm{Y}}, \quad 0 < \tau < \tau_{\max} \tag{24}$$

Here time τ is the residence time, i.e. the time during which an element of the liquid with volume dV has been in the module. The maximum residence time therefore is

$$\tau_{max} = \frac{V}{\Omega} \tag{25}$$

where V is the overall volume of the liquid in a module.
Combining eqns. (23a,b) and eqn. (24) we get

$$0 = D_M \frac{\partial^2 C_M}{\partial x_M^2}, \quad 0 < x_M < h_M \tag{26a}$$

$$\frac{\partial C_1}{\partial \tau} = D_1 \frac{\partial^2 C_1}{\partial x_1^2}, \quad 0 < x_1 < h_1 \tag{26b}$$

Equation (26a) means that the penetrant concentration distribution is linear across both of the polymeric membranes, so diffusion in the three layered medium can be considered as a diffusion in a single liquid layer with linear 3rd order boundary conditions.

Finally, in order to get concentration distributions across the module in the x direction we need to solve the Fick's equation (26b) with boundary conditions

$$-D_1 \left.\frac{\partial C}{\partial x}\right|_{x_1=0} = -\chi[\sigma_1 p_0 - C_1(0,\tau)] \tag{27a}$$

$$-D_1 \left.\frac{\partial C}{\partial x}\right|_{x_1=h_1} = \chi[\sigma_1 p_0 - C_1(h_1,\tau)] \tag{27b}$$

and initial condition

$$C_1(x_1,0)=C_{1o} \tag{28}$$

where $C_1(0,\tau)$, $C_1(h_1,\tau)$ are concentrations on the boundaries of the liquid and $\chi=D_M/h_M$.

It is possible to derive an analytical solution of eqn. (26b) with boundary conditions (27a,b) and initial condition (28) [12]

$$\frac{C_1(x_1,\tau)-C_{1o}}{\sigma_1 p_0 - C_{1o}} = 1 - \sum_{m=1}^{\infty} \frac{2F \cos\frac{2\beta_m x_1}{h_1} \exp\left(-\frac{4\beta_m^2 D_1 \tau}{h_1^2}\right)}{(\beta_m^2 + F^2 + F)\cos\beta_m} \tag{29}$$

where the β_m are the positive roots of the transcendental equation

$$\beta_m \tan(\beta_m)=F; \quad F = \frac{h_1 \chi}{2D_1} \tag{30}$$

If $\sigma_1 p_o > C_{lo}$, expression (29) will describe the concentration profiles in the absorption module. Correspondingly, if $C_{lo} > \sigma_1 p_0$, expression (29) will be valid for the desorption module. Penetrant flow rate, entering or leaving the module, can be determined in accordance with:
Absorption module

$$J_a = \left[C_{1o,a} - \frac{\int_0^{h_1} C_1(x_1,\tau)\,dx_1\big|_{\tau=L_a/\theta_Y}}{h_1} \right] \Omega \tag{31}$$

Desorption module

$$J_d = \left[C_{1o,d} - \frac{\int_0^{h_1} C_1(x_1,\tau)\,dx_1\big|_{\tau=L_d/\theta_Y}}{h_1} \right] \Omega \tag{32}$$

Continuous flow membrane absorber

In a continuous flow membrane absorber the following boundary conditions hold

$$C_{1o,a}=C_{1o} \tag{33a}$$

$$C_{1o,d}=\frac{\int_0^{h_1} C_1(x_1,\tau)\,dx_1\big|_{\tau=L_a/\theta_Y}}{h_1} \tag{33b}$$

Overall penetrant flow rate at the desorber outlet will be equal to J_d. For a continuous flow membrane absorber

$$|J_a|>|J_d| \tag{34}$$

Circulatory membrane absorber

In a circulatory membrane absorber the boundary conditions are

$$C_{1o,d}=\int_0^{h_1} C_1(x_1,\tau)\,dx_1\big|_{\tau=L_a/\theta_Y} \tag{35a}$$

$$C_{1o,a}=\int_0^{h_1} C_1(x_1,\tau)\,dx_1\big|_{\tau=L_d/\theta_Y} \tag{35b}$$

For a circulatory membrane absorber

$$|J_a|=|J_d| \tag{36}$$

Solutions for eqns. (31) and (32) with the boundary conditions (35) were obtained by the method of iterations. The system of eqns. (22) is a more general approach to the problem. At $\sigma_1 D_1/h_1 \gg \sigma_M D_M/h_M$ it will yield eqns. (9) and (16) as the concentration profile of the penetrant across the liquid will be almost linear. In this case the assumptions made for the plug-flow model will be valid. It should be mentioned that the plug-flow regime is the most effective regime in which a membrane absorber can operate.

Calculation algorithm

The following procedure was employed to calculate the transmembrane flux in the circulatory membrane absorber.

- Step 1. For a given flow rate Ω and module geometry the maximum residence time τ_{max} is calculated according to eqn. (25). Calculations begin with the absorber module.
- Step 2. An initial concentration of penetrant across the absorbent layer is assumed: $C_1(x_1,0) = C_{1o}$.
- Step 3. The concentration distribution is calculated in accordance with eqn. (29) at time τ_{max} across the liquid layer (e.g. at 20 points along the x-axis).
- Step 4. The penetrant concentrations are summed across the c-axis (at 20 points) and divided by the number of points to get the average concentration at the module outlet which will be used as the inlet concentration C_{1o} in the next module.
- Step 5. Total transmembrane flow rate into/from the absorption liquid is calculated as the difference between the average inlet and outlet penetrant concentrations multiplied by the volumetric liquid flow rate.
- Step 6. Steps 2 to 4 are repeated to get the distribution of concentration at the desorber module outlet.
- Step 7. Total transmembrane flow rate at the desorber outlet is calculated as the difference between the average inlet and outlet concentrations in the desorber module multiplied by the volumetric liquid flow rate.
- Step 8. Steps 2 to Tare repeated until the condition for convergence (36) is satisfied.

(4) Recommendations

The analysis performed above is for the flat sheet membrane module configuration. At the same time it is obvious that the conclusions drawn from the model will be valid for the hollow fiber membrane module as well. The following recommendations are proposed for the design of a pilot scale installation. To prevent concentration-polarization, stirring of the liquid layer should be provided. One may also reduce the diffusion

resistance of the liquid layer by decreasing its thickness. From our preliminary calculations it follows that a thickness of the liquid layer equal to 50 μm could provide 70-80% of the membrane absorber productivity in the plug-flow regime. Therefore, it is advantageous to use hollow fiber membranes as it is relatively easy to obtain hollow fiber membranes with an inner diameter of approximately 50 μm. At the same time, the hollow fiber module is the most effective one for a membrane absorber design because it provides the highest values of surface area to equipment volume ratio. It is noteworthy that at the present time the hollow fiber membrane module has one of the highest surface area to equipment volume ratios known for technological devices, even though it is still much less than for animal lungs. The absorbent flow rate should not be too high as this will lead to a decrease in the selectivity of the separation. It follows from the mathematical analysis, that at a low pumping rate of the absorbent the nature of the membrane has almost no influence on the productivity and selectivity of the device. Consequently, in this regime microporous and nonselective membranes made of hydrophobic polymers can be employed for membrane absorber design. Such a device will combine a high selectivity of the absorption process with the maintenance of a high value of surface area to equipment volume ratio typical for membrane devices.

Experimental

Materials

Flat sheet polyvinyltrimethylsilane (PVTMS) asymmetric membranes were used in all experimental investigations reported in this study. The thickness of the dense skin layer was approximately h_M = 0.1 μm. Distilled water, 10 vol.% and 20 vol.% aqueous solutions of monoethanolamine (MEA) were chosen as absorption liquids. All the permeation experiments were performed with a binary gas mixture CO_2/CH_4 with composition 53/47. In the desorption module He (99.99% purity) was admitted as a carrier gas.

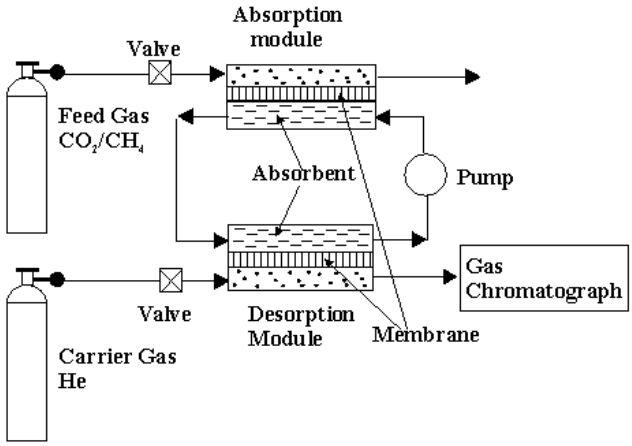

Fig. 4. Schematic of experimental installation.

Experimental Installation

Experimental set-up

A schematic of the experimental installation used for the laboratory gas separation of CO_2/ CH., is presented in Fig. 4. The circulatory membrane absorber was composed of two membrane cells with a membrane surface area equal to 28.3 cm^2 each. The absorption liquid thickness under the membrane was equal to h_1=1 mm. In the absorption module a CO_2/CH_4 mixture of gases was used as a feed. The absolute pressures of the gas mixture and purge gas were kept constant at atmospheric pressure in both absorption and desorption modules. A gas chromatograph was used to check the composition of the gas mixture at the desorption module outlet. Absorption liquid was fed using a peristaltic pump. In this particular experimental set-up it usually took 10 to 24 hr for the system to reach steady state.

Results and discussion

The performance of the membrane absorption system was determined by using the experimental circulatory membrane absorber described previously for the separation of a CO_2/ CH_4 gas mixture. The main objective was to establish the validity of the theoretical models proposed for the description of the gas separation properties of the membrane absorber integrated system.

As expected from the theoretical simulations, with increasing absorbent flow rate the permeation rates were increasing for both CH_4 and CO_2 (Figs. 5, 6) while the selectivity factors were simultaneously decreasing (Figs. 7, 8). If pure water was used as the absorption liquid, the maximum selectivity coefficient achieved was 91 at the absorbent flow rate Ω=0.024 cm^3/sec. This value was more than 3 times higher than the selectivity of solubility $\alpha_\sigma=\sigma(CO_2)/\sigma(OH_4)$ = 25 calculated from the solubility coefficients of pure CO_2 and CH_4 in water.

This fact can be explained if the salting out effect is taken into consideration (at p_{CO_2} = l atm, T=20°C, pH = 4). It is a well-known phenomenon that the solubility coefficient of CH_4 decreases in ionic solutions. A decrease in CH_4 solubility resulted in an increase of the membrane absorber selectivity. At high liquid flow rates the influence of the solubility coefficients on the total transmembrane flow rate is not significant. The selectivity in this case is determined mainly by the selectivity of the polymeric membrane itself, as can be seen in Fig. 7.

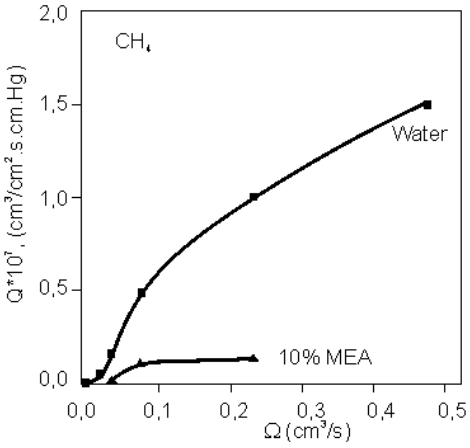

Fig. 5. CH_4 productivity in a circulatory membrane absorber via absorbent flow rate.

It is reasonable to expect an increase in the selectivity coefficients, if solutions of complex binders, able to reversibly form complex compounds with one of the components of the gas mixture, are used as absorbents.

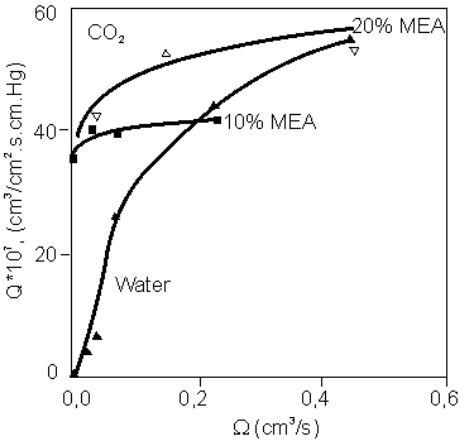

Fig. 6. CO_2 productivity in a circulatory membrane absorber via absorbent flow rate.

In our experiments we used monoethanolamine (MEA) as a complex binder for selective CO_2 absorption. The results obtained are presented in Figs. 5 and 6. Selectivity factors as high as 3500 were observed when a 10 vol.% solution of MEA was used as the absorption liquid (Fig. 8). There are two facts influencing the selectivity factor in this case. First, the permeation rate of CO_2 increases, due to the facilitation factor, and the CO_2 solubility increases, due to changes in the pH of the solution caused by the presence of MEA. Second, the solubility of CH_4 decreases due to the salting-out effect. Thus, the separation performance was influenced by two factors acting in opposite directions that resulted in very high selectivity factors for CO_2/CH_4 gas mixture separation.

A further increase in the concentration of MEA in water (from 10 vol.% to 20 vol.%) only slightly influenced the permeation rates of CO_2, whereas the selectivity factors increased even more as we were not able to detect the permeation rates of CH_4 using a GC. This observation means that the increase in the selectivity of gas separation in this case was mainly due to the decrease of the solubility coefficient of CH_4, rather than due to an increase in the CO_2 permeability due to the facilitation factor.

The comparison between the experimental data for CO_2 permeability and the simulation results in a membrane absorber with water used as the absorption liquid are presented in Fig. 9. One may see that the discrepancies between the plug-flow model predictions and the experimental data are significant since the thickness of the absorption liquid in our experimental setup was equal to 1 mm. When the thickness of the absorption liquid is considerable, concentration-polarization may play an important role in decreasing the overall transmembrane flux in the membrane absorber. The lamellar medium model of gas desorption with the 3rd order boundary conditions gives more reasonable predictions, but the simulated CO_2 productivity is still higher than the experimental measurements. A possible explanation of this discrepancy between the theoretical curve and experimental results could be the existence of a non-linear profile of the liquid flow rate in the absorption/desorption modules. This would result in an even stronger influence of concentration-polarization on the transmembrane fluxes of gases.

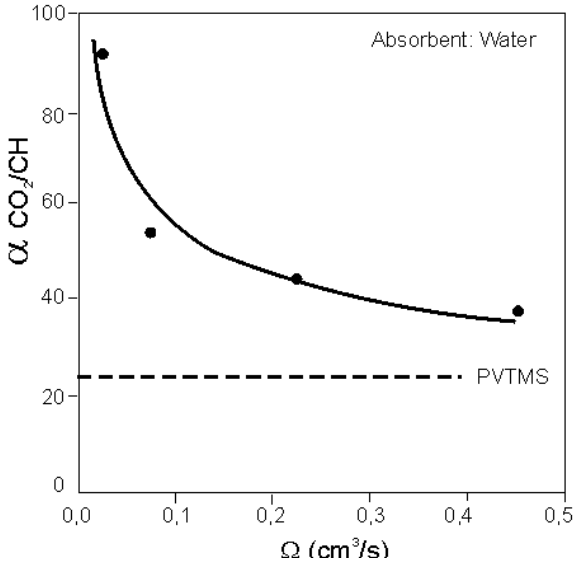

Fig. 7. CO_2/CH_4 selectivity factors in a circulatory membrane absorber via water flow rate.

Thus, we may conclude that in order to increase the productivity of the membrane absorber, we have to decrease the thickness of the absorption liquid layer as much as possible. The creation of conditions at which flow of the absorbent will be turbulent will also favor an increase of the transmembrane flux; this however, can be achieved only at high liquid flow rates when the selectivity of the process is minimal.

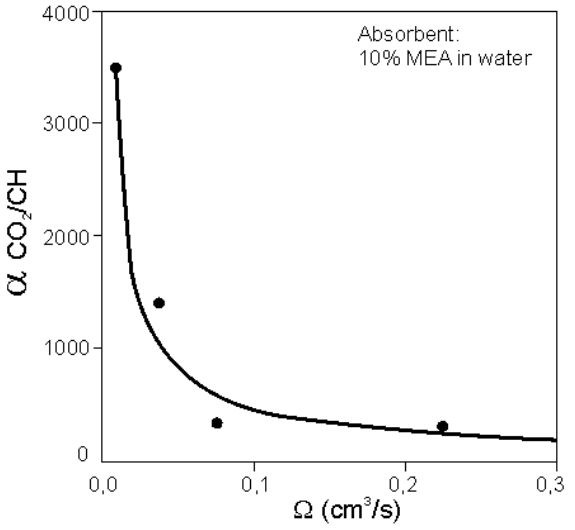

Fig. 8. CO_2/CH_4 selectivity factors in a circulatory membrane absorber via 10% monoethanolamine solution flow rate.

Conclusions

By combining membrane and absorption separation process in a single device called a membrane absorber, it is possible to unite the advantages of both within one technological unit. A very high ratio of absorbent surface area to module volume can be achieved by pumping the absorbent in a hollow fiber membrane module. The selectivity and productivity of the separation process can be controlled in such a device, allowing one to adjust its properties to operational conditions without process interruption. There will also be a considerable decrease in hazardous exhausts of absorbent from both absorption and desorption modules.

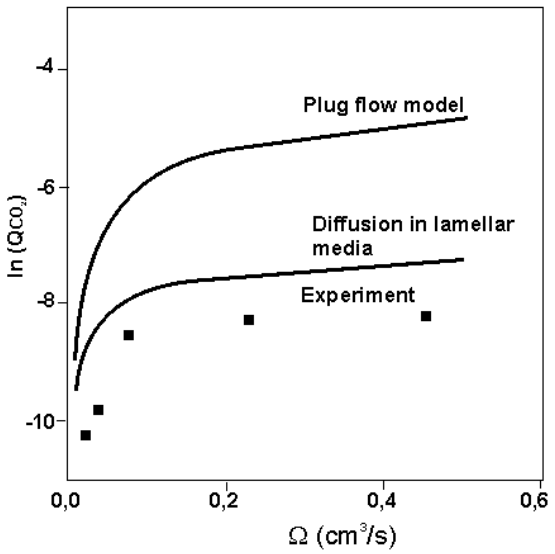

Fig. 9. Comparison between the experimental data for CO_2 permeability and simulation results for circulatory membrane absorber.

List of symbols

A	dimensionless constant
C	concentration [cm^3(STP)/cm^3]
D	diffusion coefficient (cm^2/sec)
F	dimensionless parameter
h	thickness (cm)
J	total transmembrane flow rate (cm^3/sec)
K	constant
L	length (cm)
p_0	pressure in gas phase (cmHg)
Q	membrane productivity [cm^3(STP)/cm^2-sec-cmHg]
S	membrane area (cm^2)
x ,y	axis

Greek letters

σ	solubility coefficient [cm^3(STP)/cm^3-cmHg]
Ω	liquid flow rate (cm^3/sec)
α	selectivity factor
ξ	dimensionless distance
θ	velocity (cm/sec)
τ	residence time (sec)
χ	diffusion resistivity (cm/sec)
ψ	dimensionless concentration

Subscript

1	liquid
M	membrane

Superscript

a	absorption module
d	desorption module
A, B	gas mixture components

References

1 W.J. Ward, III, Analytical and experimental studies of facilitated transport, AIChE J., 16 (1970) 405.

2 S.L. Matson, C.S. Herrick and W.J. Ward, III, Progress on the selective removal of H_2S from gasified coalusing an immobilized liquid membrane, Ind. Eng. Chem., Process Des. Dev., 16 (1977) 370.

3 W.J. Ward, Immobilized liquid membranes, in N.N. Li (Ed.), Recent Developments in Separation Science, CRC Press, Boca Raton, FL, 1972.

4 K.K. Sirkar, Selective permeation gas separation process and apparatus, Patent U.S.A., 4750918,1988.

5 A.K. Guha, S. Majumdar and K.K. Sirkar, Gas separation modes in a hollow fiber contained liquid membrane permeator, Ind. Eng. Chem. Res., 31 (1992) 593.

6 M. Teramoto, H. Matsuyama, T. Yamashiro and S. Okamoto, Separation of ethylene from ethane by flowing liquid membrane using silver nitrate as a carrier, J. Membrane Sci., 45 (1989) 115.

7 7. A.B. Sholekhin, Diffusion separation of gases in membrane absorption heterogeneous systems, Ph.D. Thesis, Moscow State University, Moscow, 1990.

8 A.B. Shelekhin and I.N. Beckman, Ideal model for gas separation processes in membrane absorber, Proc. Int. Congress of Membranes and Membrane Processes, ICOM-90, Chicago, Vol. 2, 1990, pp. 1419-1421.

9 A.B. Shelekhin, I.N. Beckman, V.V. Teplyakov and I.N. Gladkov, The method of membrane gas mixture separation, USSR Patent 1637850, 1989.

10 P.II Mancini, G.C. Whittlesey, C Grant, J.Y. Song, S.O. Salley and M.D. Klein, CO_2 removal for ventilatory support. A comparison of dialysis with and with out carbonic anhydrase to a hollow fiber lung, ASAIO Transactions (American society for Artificial Internal Organs), 36 (1990)675-678.

11 M.-C. Yang and E.L. Cussler, Artificial gills, J. Membrane Sci., 42 (1989) 273-284.

12 J. Crank, The Mathematics of Diffusion, Clarendon Press, Oxford, 1956, p. 347.